Applied Environmental Research
- RESEARCH FOR SUSTAINABLE PLANET -

Research Article

# Low-temperature Catalytic Oxidation of White Spirit Vapor in Air by Binary Oxides of FeO-$MnO_x$ Supported on OMS-2 Material

**Ngo Quoc Nguyen[1,2], Pham Duy Quang[1,2], Nguyen Ha Nhu[1,2], Le Thi Van Anh[1,2], Nguyen Thi Thuy[2,3], Vo Thanh Hang[1,2], Le Van Thang[2,3], Nguyen Thi Le Lien[2,4], Nguyen Trung Thanh[2,5], Nguyen Nhat Huy[1,2,*]**

[1] *Faculty of Environment and Natural Resources, Ho Chi Minh City University of Technology (HCMUT), 268 Ly Thuong Kiet St., Dist. 10, Ho Chi Minh City, Vietnam*
[2] *Vietnam National University Ho Chi Minh City, Linh Trung Ward, Thu Duc City, Ho Chi Minh City, Vietnam*
[3] *School of Chemical and Environmental Engineering, International University, Linh Trung Ward, Thu Duc City, Ho Chi Minh City, Vietnam*
[4] *Faculty of Chemical Engineering, Ho Chi Minh City University of Technology (HCMUT), 268 Ly Thuong Kiet St., Dist. 10, Ho Chi Minh City, Vietnam*
[5] *Laboratory of Nanomaterial, An Giang University, 18 Ung Van Khiem St., Dong Xuyen Ward, Long Xuyen City, An Giang Province, Vietnam*

*Corresponding Email: nnhuy@hcmut.edu.vn

## Abstract

In this work, catalysts of iron and manganese oxides supported on OMS-2 were prepared and applied to remove white spirit (WS) in air. Among the fabricated catalysts, the FeO-$MnO_x$/OMS-2 catalyst with a surface Fe+Mn loading of 15% (Fe:Mn = 6:4) exhibited the highest catalytic performance, achieving a high WS removal efficiency of 97.91% at 200 °C. The catalyst retained the cryptomelane-type tunnel structure of OMS-2 and possessed enhanced redox activity due to the synergistic interaction between surface Fe and Mn species. The physico-chemical properties were characterized via BET, EDS, FTIR, XRD, and SEM. The suitable conditions for WS oxidation were identified as 1 g of catalyst, a 1 L $min^{-1}$ gas flow rate, and a maximum inlet concentration of 2000 ppm at a low operating temperature of 200 °C. While the catalyst proved highly effective in WS treatment, durability tests indicated performance degradation over prolonged use, highlighting a direction for future enhancement.

**ARTICLE HISTORY**

Received: 11 Mar. 2025
Accepted: 11 Jun. 2025
Published: 18 Jun. 2025

**KEYWORDS**

White spirit;
Catalytic oxidation;
OMS-2;
Binary oxides

## Introduction

Transition metal oxides and noble metal catalysts (mainly Pt and Pd) are the two main materials used in many studies for removing volatile organic compounds (VOCs) in air. In some cases, transition metal oxide-based catalysts function similarly to $Pt/Al_2O_3$ catalysts, are less costly than noble metal catalysts, and are typically more poisoning resistant [1–3]. They often contain two or three types of metals and may also have a significantly larger surface area. Consequently, much research has been conducted on transition metal oxides as more effective and affordable catalysts for the total oxidation of VOCs. Several metal oxide catalysts have been evaluated for the oxidation of VOCs, including single metal oxides (e.g., Cu, Mn, Ce, Ni, Co, Mo, Zr, Cr, V, and Fe) and their binary forms [4–5]. The ability of these materials to completely oxidize VOCs is usually influenced by the type of VOC as well as the properties and morphology of the catalysts and carriers.

White spirit (WS) is a complex mixture composed of both aliphatic and aromatic hydrocarbons (e.g., toluene, benzene, and n-hexane), which are highly volatile, toxic, and persistent in the environment [6]. Chronic exposure to WS is frequently linked to adverse health effects, including neurotoxicity, respiratory irritation, and potential carcinogenicity. Conventional VOC abatement technologies (e.g., thermal incineration, adsorption, and biofiltration) often encounter significant limitations related to high energy consumption, complicated regeneration processes, and solid waste generation. Thermal incineration is highly effective in decomposing VOCs but requires very high operating temperatures of 600–1000 °C, leading to high energy consumption and treated flue gas cooling requirements [7]. Adsorption using activated

https://doi.org/10.35762/AER.2025022

carbon allows simpler operation at ambient temperature but is limited by low capacity, saturation effects, and the need for frequent adsorbent regeneration. Biofiltration is environmentally friendly and suitable for biodegradable VOCs at low concentrations; however, it suffers from a slow response time, dependency on microbial stability, poor efficiency for biotoxic or hydrophobic compounds, and ineffectiveness for VOCs at high concentrations.

To overcome these drawbacks, catalytic oxidation has emerged as a promising alternative, offering complete conversion of VOCs into $CO_2$ and $H_2O$ under relatively low operating temperatures of 150–350 °C with high selectivity, long-term stability, and low energy demand. Therefore, it is highly suitable for treating complex organic mixtures such as WS, which contains both aromatic and aliphatic hydrocarbons with high volatility and toxicity. In this context, catalytic oxidation was selected to treat WS vapor due to its superior efficiency and environmental compatibility, aiming to develop a cost-effective, low-temperature catalytic system using transition metal oxides supported on OMS-2. In addition, recent works have demonstrated that transition metal oxide catalysts (particularly those containing Cu, Mn, or Fe) exhibit notable activity in the oxidation of individual VOC components typically found in WS mixtures [8–11].

Additionally, the ability of an oxide material to oxidize VOCs at a certain temperature depends on the metal composition, surface area, and structure, in which composite oxides are often better than single oxides [12]. To produce effective catalysts for VOC treatment, several carriers, such as $MnO_2$, $TiO_2$, $CeO_2$, γ-$Al_2O_3$, and OMS-2, have been used to maximize the exposure of the catalysts on their surface [2, 3, 13–14]. Because of its nanostructure with a large specific surface area, γ-$Al_2O_3$ is currently the subject of much research as a carrier to support other metal oxides. Gas molecules can penetrate deeply into the pore network and access the internal surface of the material, where the metal oxide catalyst is present. Additionally, both γ-$Al_2O_3$ and $MnO_2$ exhibit high thermal stability, which helps prevent sintering and agglomeration of the catalysts during operation [15]. Metal oxides of CuO, $CeO_2$, and $MnO_2$ and a mixture of these oxides impregnated onto γ-$Al_2O_3$ were prepared to treat toluene gas, and the most effective catalyst was 30MnO-50$CeO_2$, with a toluene conversion of over 97% at 280 °C [12]. On the other hand, CuO/γ-$Al_2O_3$ or CuO-$CeO_2$/γ-$Al_2O_3$ had a treatment efficiency of at least 90% for toluene above 250 °C, whereas $CeO_2$/γ-$Al_2O_3$ needed 350 °C to reach the same efficiency [12]. In another study, when CuO was combined with different supports (e.g., $CeO_2$, γ-$Al_2O_3$, $TiO_2$, and $V_2O_5$), the CuO/$CeO_2$ catalyst exhibited the best toluene oxidation efficiency of 90% at 315 °C [16].

Manganese-based oxides are among the most extensively studied catalysts for the removal of gaseous pollutants because of their various oxidation states, environmental compatibility, and cost effectiveness. Depending on the synthesis conditions, manganese oxides can exist in multiple oxidation states and crystalline phases, such as MnO, $Mn_2O_3$, $Mn_3O_4$, and $MnO_2$, each of which contributes differently to the catalytic performance. The catalytic activity of these materials is governed by key physicochemical properties, such as their crystal structure, morphology, surface area, and particle size [17]. The abundance of lattice oxygen contributes to structural instability. This facilitates the incorporation and mobility of oxygen within the crystal lattice, thereby enhancing the oxidation of VOCs and CO. The effectiveness of eliminating VOCs (e.g., ethyl acetate, benzene, and toluene) has been the subject of several recent studies [8, 12, 18–20]. The catalyst synthesis method, catalytic experimental conditions, and oxidation state of manganese determine the effectiveness of the oxidation process using manganese oxide because of the presence of $Mn^{3+}/Mn^{2+}$ and $Mn^{4+}/Mn^{3+}$ redox pairs [5]. Furthermore, the Mn-based catalyst demonstrated even higher activity than the Pt/$TiO_2$ catalyst in the oxidation of n-hexane and ethyl acetate [1, 2, 20].

Additionally, to increase the catalytic activity, some researchers have focused on the combination of manganese oxide and other transition metal oxides. A Cu–Mn oxide catalyst was used to oxidize CO and VOCs at room temperature with high efficiency [14, 20–22]. Cu–Mn oxide composites have also been investigated for propane oxidation, and they are more effective than single manganese or copper oxides at lower temperatures [23]. Furthermore, the presence of Cu reduces the surface area but increases the porosity of $MnO_2$, thereby affecting the oxidation activity of the catalyst [24]. Different VOCs (e.g., toluene, benzene, ethylbenzene, and xylene) are oxidized by the Cu–Mn oxide catalyst, which has the highest removal efficiency for toluene [4]. Carrier-supported catalysts have also been studied and used in industry in several studies [25]. $CuMnO_x$ supported on $SiO_2$ was prepared, and the $CuMn_2O_4$ and $Cu_2Mn_3O_8$ phases exhibited the highest activity in the oxidation of benzene [5]. In addition, adding Cu and Mn oxide particles to SBA-15 also increased the catalyst activity for ethyl acetate oxidation [26].

OMS-2 is a specific type of cryptomelane α-$MnO_2$ that features a distinctive 2×2 tunnel structure built from corner- and edge-sharing [$MnO_6$] octahedra. While α-$MnO_2$ refers to a broader tetragonal polymorph of manganese dioxide, OMS-2 represents a more well-defined, defect-free, and ordered form than does α-$MnO_2$, in which K+ ions and water molecules reside within the tunnels to maintain charge balance and framework stability [27]. In addition, OMS-2 contains Mn in multiple oxidation states (e.g., $Mn^{2+}$, $Mn^{3+}$, and $Mn^{4+}$), endowing it with enhanced redox behavior and ion-exchange capabilities. In addition, its moderate surface acidity

and mesoporous structure further support its catalytic oxidation ability.

Iron-based catalysts, particularly Fe-containing binary oxides, have emerged as promising materials for VOC oxidation because of their favorable redox properties, low cost, and environmental compatibility. Previous studies have demonstrated that Fe-based catalysts exhibit competitive or even superior activity compared with noble or other transition metal oxides. For example, the $Fe_2O_3$-$MnO_x$ composite demonstrated high catalytic efficiency in toluene oxidation due to the synergistic interaction between Fe and Mn species, which enhances oxygen mobility and redox cycling [28]. Similarly, Fe-doped OMS-2 materials improved the redox capacity and structural stability of the manganese oxide framework under thermal and reaction conditions for the effective oxidation of toluene, acetone, and dichloromethane [8]. These findings support the strategic selection of FeO-MnO/OMS-2 as a robust catalytic material for the treatment of VOCs, such as WS.

In this study, OMS-2 was synthesized via the hydrothermal method, while FeO/OMS-2 and FeO-$MnO_x$/OMS-2 were further prepared by incorporating Fe and Mn oxides on the surface of OMS-2 via the impregnation method. The materials were then characterized via techniques such as BET, XRD, FTIR, SEM, and EDS. The catalytic performance of these materials was evaluated for the oxidation of WS vapor under various operating conditions, including different temperatures, gas hourly space velocities (GHSV), WS concentrations, and catalyst dosages. Furthermore, catalyst durability was also investigated to assess its potential for real-world application in VOC abatement systems.

## Methods

### 1) Catalyst preparation and characterization

In this work, three different catalysts were studied, including OMS-2, FeO-OMS-2, and FeO-$MnO_x$/OMS-2. OMS-2 was prepared via a hydrothermal method [29]. First, 11.33 g of $MnSO_4$ was added. $H_2O$ and 7.57 g of $KMnO_4$ were dissolved in 158 mL of distilled water. Next, the solution was acidified with 4 mL of concentrated $HNO_3$, stirred vigorously for 30 min, and then subjected to ultrasonication for an additional 30 min. The mixture was then hydrothermally treated at 160 °C for 24 h. After treatment, the mixture was subjected to filtration and rinsed with distilled water until a neutral pH was reached. Finally, the product was dried at 120 °C for 12 h, followed by calcination in air at 400 °C for 6 h. For the FeO/OMS-2 catalyst, the uncalcinated OMS-2 was mixed with a mixture of $FeSO_4 \cdot 7H_2O$ salt with a theoretical Fe:Mn molar ratio of 15%. Then, a sufficient amount of water was added to the mixture and stirred for 30 min. After stirring, the mixture was dried at 100 °C for 24 h to completely evaporate the water in the mixture. Finally, the mixture was calcined at 400 °C for 6 h to produce OMS-2. With the FeO-$MnO_x$/OMS-2 catalyst, both $FeSO_4 \cdot 7H_2O$ and $MnSO_4 \cdot H_2O$ (with a theoretical Fe:Mn molar ratio of 6:4) was added to OMS-2 (with a theoretical molar ratio of 15% for Fe+Mn on the surface to Mn in OMS-2).

The specific surface area of the materials was measured through $N_2$ adsorption–desorption via the Brunauer–Emmett–Teller (BET) and Barrett–Joyner–Halenda (BJH) methods via a PMI BET–201A sorptometer. The crystallinity of the materials was analyzed with a Bruker D2 Phaser X-ray diffractometer (XRD) using CuKα radiation with a 2θ angle range of 5° to 80°. The morphology of the catalysts was examined via a JEOL JSM-IT200 high-resolution scanning electron microscope (SEM). The surface species on the catalyst were characterized via a Bruker Alpha II Fourier transform infrared (FTIR) spectrometer.

### 2) Catalytic tests

Figure 1 shows a schematic diagram of the experimental model, which consists of three parts: (i) a gas supply, (ii) a fixed-bed reactor, and (iii) a sampling and analysis system. In the gas supply system, an air pump equipped with an air cleaner was used to supply zero air for the system, and the flow rate was controlled by a mass flow controller (MFC). The air stream is then split into two separate streams: one passes through an MFC into a bubbler containing WS solvent to produce a WS-containing gas, and the other goes directly to a chamber for mixing before being introduced to the reactor. The reactor is made of a straight tube containing the catalyst (1 g, particle size of 20–40 mesh) and support material (glass wool). This reactor is heated and stabilized by a temperature regulator, which can adjust the temperature from 25 to 250 °C depending on the required temperature.

The WS concentration was sampled and determined according to a method developed by Olkhovskaya [30]. The absorbance was analyzed with a spectrophotometer (Hach DR 5000). All experiments were repeated in triplicate, and the average values and error bars are displayed in the charts.

The conversion of WS is calculated via the following equation (Eq.1).

$$H(\%) = \frac{C_i - C_o}{C_i} \times 100\% \qquad \text{(Eq. 1)}$$

Where H is the WS conversion (%) and $C_i$ and $C_o$ are the WS concentrations at the inlet and outlet (ppm), respectively.

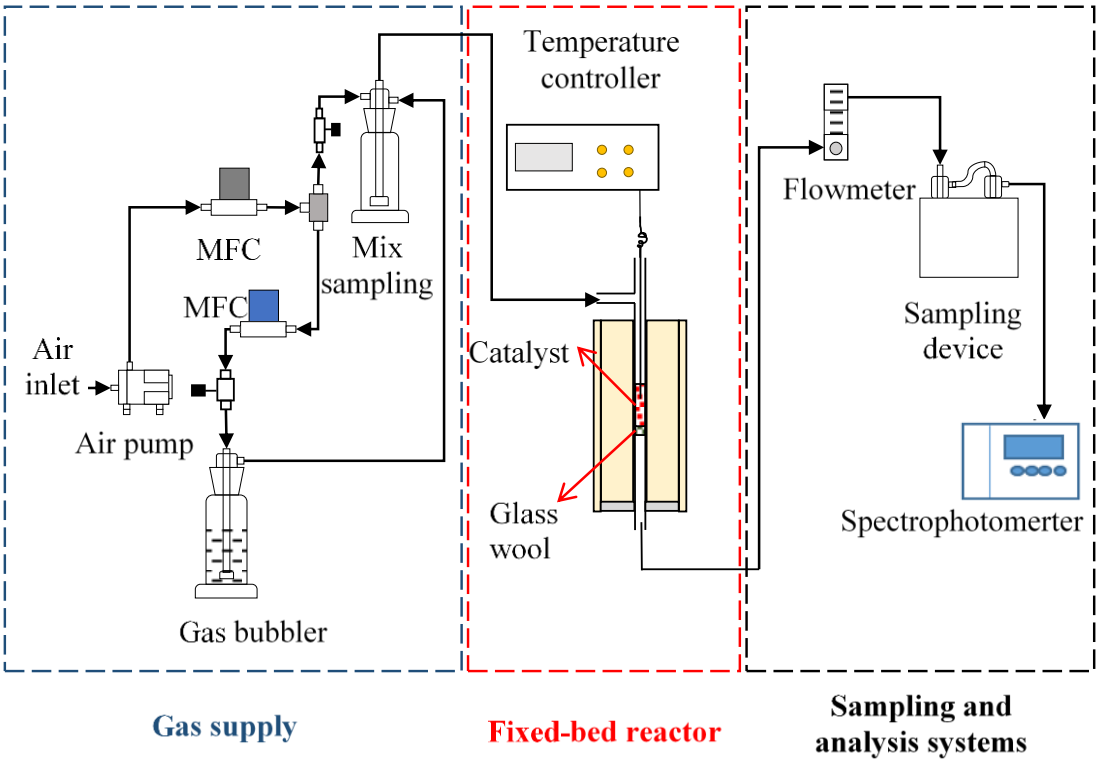


**Figure 1** Lab-scale model for measuring the catalytic activity.

## Results and discussion

### 1) Structural properties and morphology of the catalysts

SEM analysis of the material morphology in Figure 2(a-b) reveals that both the OMS-2 and fresh FeO-$MnO_x$/OMS-2 catalysts exhibit a distinct and consistent rod-like microstructure, a feature commonly linked to elevated catalytic activity. This also illustrates that the FeO-$MnO_x$/OMS-2 material has a greater nanorod composition, accompanied by the existence of Fe and Mn oxides on the surface of the OMS-2 support. The chemical compositions of the OMS-2 and FeO-$MnO_x$/OMS-2 materials were measured via EDX analysis, as shown in Figure 2(c-d). In both samples, the higher contents of Mn and O indicate that the main components of the hydrothermally synthesized OMS-2 nanorods are Mn and O. In the FeO-$MnO_x$/OMS-2 catalyst, the peaks corresponding to the binding energy of Fe and Mn are more prominent than those in the OMS-2 material. Furthermore, the atomic percentages of the components in the FeO-$MnO_x$/OMS-2 catalyst reveal that O, Mn, and Fe constitute a significant proportion of the material.

The specific surface areas of the synthesized OMS-2 and FeO-$MnO_x$/OMS-2 catalysts were 69.88 and 64.91 $m^2\ g^{-1}$, respectively. According to the $N_2$ adsorption–desorption isotherms in Figure 2(e), both samples exhibit type IV isotherms with H3-type hysteresis loops at a relative pressure P/P0 > 0.4, indicating the presence of mesoporous structures. This porous structure facilitates the diffusion and adsorption of VOCs with medium to large molecular sizes. The BJH pore size distribution curves in Figure 2(f) further reveal that both catalysts possess a dominant mesoporous structure with pore sizes mainly distributed in the 20–50 Å range, accompanied by a negligible fraction of micropores. Notably, compared with OMS-2, FeO-$MnO_x$/OMS-2 presented a slightly narrower pore size distribution and lower pore volume in the mesopore region, suggesting that the incorporation of Fe and Mn oxides may partially block or alter the channel structure of OMS-2. Despite this, FeO-$MnO_x$/OMS-2 retained a high surface area and accessible porous structure, making it suitable for catalytic applications involving gaseous pollutants.

The crystal phase and crystallinity of the produced materials were examined via X-ray diffraction (XRD) over a 2θ range of 10° to 80° at a scanning rate of 0.02°/s. As observed in Figure 3(a), the peaks found at 2θ values of 12.6°, 17.9°, 28.6°, 37.5°, 41.9°, 49.9°, and 60.1° confirm the characteristic pattern of cryptomelane ($KMn_8O_{16}$), thereby indicating the structural type of OMS-2 material as I4/m tetragonal, with parameters of a = b = 9.78 Å and c = 2.86 Å. In the FeO-$MnO_x$/OMS-2 material, the same peaks were found, in accordance with the crystal planes of (110), (200), (310), (211), (301), (411), and (521), thus preserving the identical cryptomelane structure and $KMn_8O_{16}$ crystalline phase as OMS-2. In addition, as plotted in Figure 3(b), the OMS-2 material had peaks at 2,361 $cm^{-1}$ (O=C=O group), 2,124–2,004 $cm^{-1}$ (N=C=N group), and 1,222–733 $cm^{-1}$ (C–O group) [31]. Similar peaks were found in the FeO-$MnO_x$/OMS-2 material at 2,355 $cm^{-1}$ (O=C=O), 2,135–1,885 $cm^{-1}$ (N=C=N), and 1,212–752 $cm^{-1}$ (C–O) [32]. There were also peaks at 1,125 $cm^{-1}$ that were related to Fe–O bond vibrations.

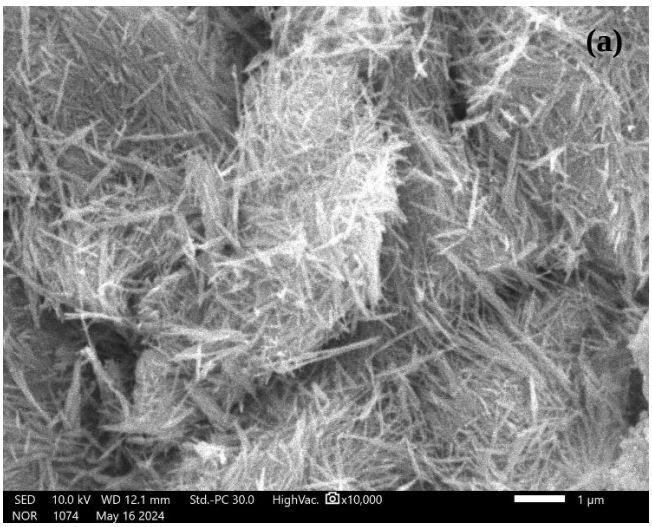


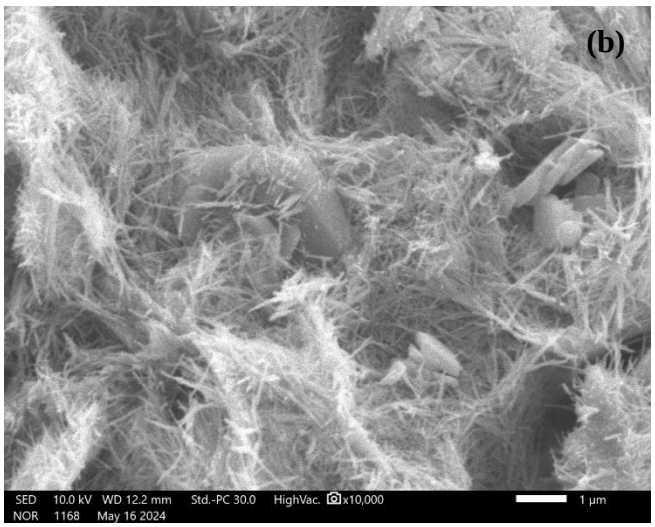


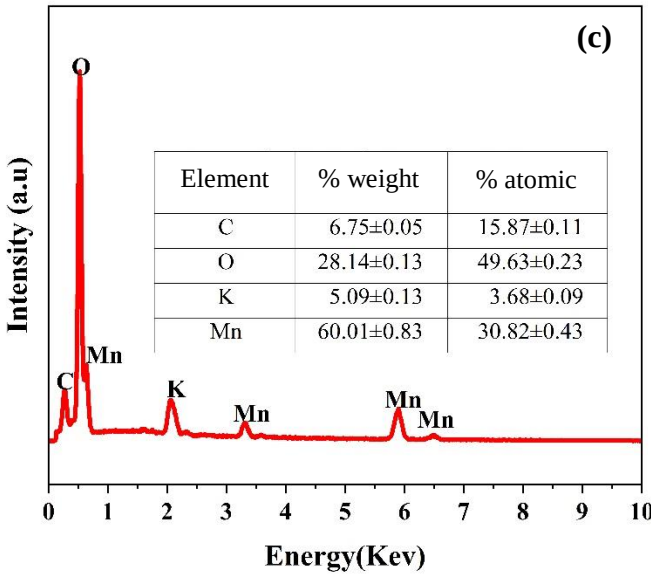


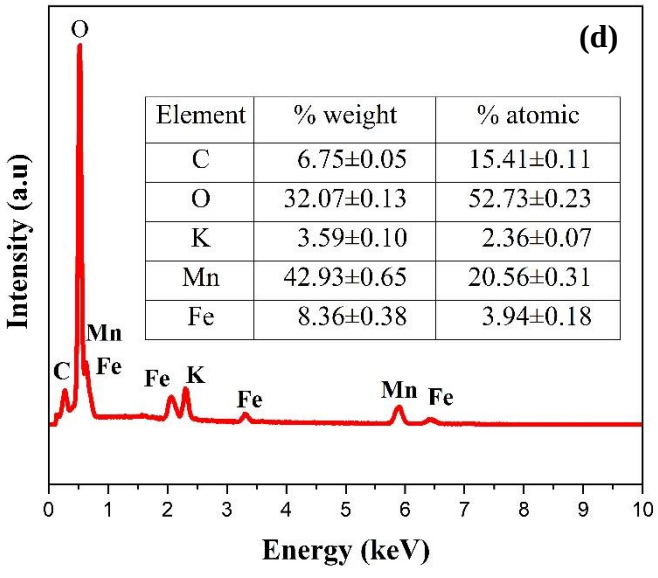


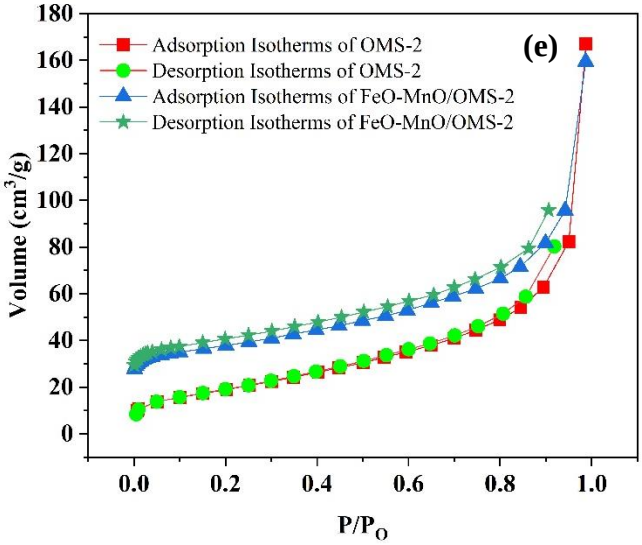


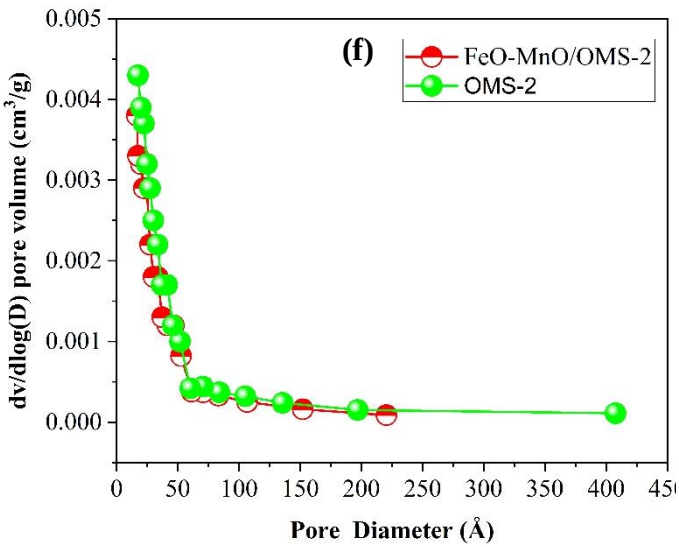


**Figure 2** SEM images of (a) OMS-2 and (b) FeO-$MnO_x$/OMS-2; EDX results of (c) OMS-2 and (d) FeO-$MnO_x$/OMS-2; (e) BET results of OMS-2 and FeO-$MnO_x$/OMS-2; and (f) pore size distribution curves of OMS-2 and FeO-$MnO_x$/OMS-2.

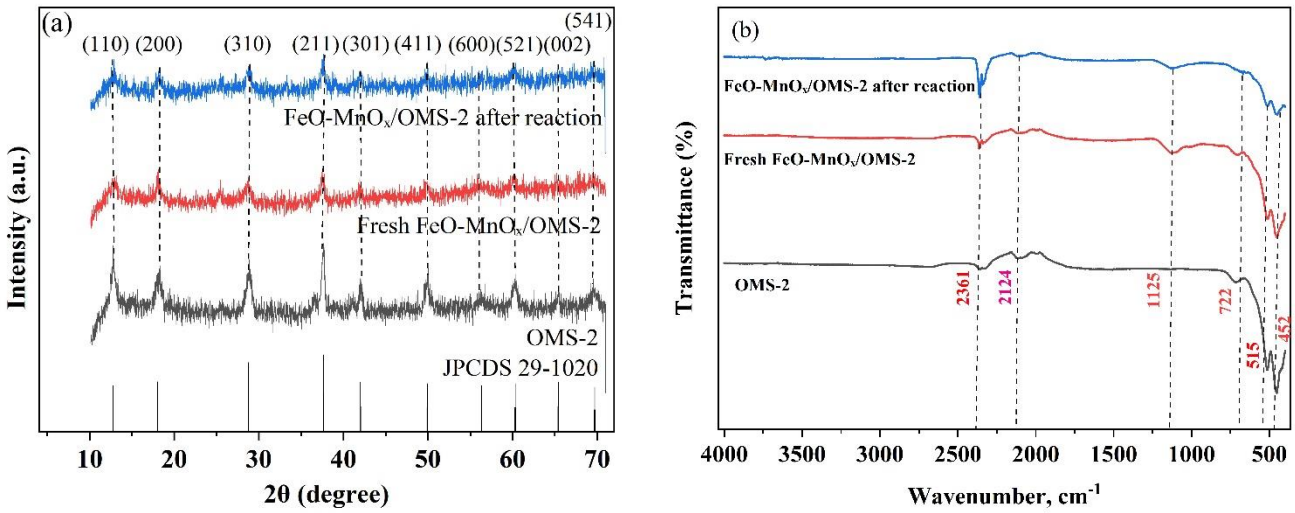


**Figure 3** Plots of (a) XRD patterns and (b) FTIR spectra of OMS-2, fresh FeO-$MnO_x$/OMS-2 and FeO-$MnO_x$/OMS-2 after the reaction.

### 2) Performance of the prepared catalysts for WS vapor oxidation

First, various catalyst materials were applied for the oxidation of WS vapor, as depicted in Figure 4(a). At temperatures above 50 °C, the efficiency of the catalysts starts to show noticeable WS removal. At 200 °C, FeO-$MnO_x$/OMS-2 exhibited excellent catalytic activity for WS, with a treatment efficiency of 98.43% and an output concentration of less than 100 ppm. Furthermore, the catalyst remained stable even as the temperature increased to 250 °C, with an efficiency of 97.6%. This was followed by the FeO/OMS-2 catalyst with an efficiency of 92.9% and the OMS-2 catalyst with an efficiency of 86.3% under similar conditions at 250 °C. The high efficiency of the FeO-$MnO_x$/OMS-2 catalyst is partially due to the preexisting redox pair of $Mn^{4+}/Mn^{3+}$ in the OMS-2-based catalyst. The incorporation of Mn and Fe oxides on the surface of OMS-2 introduces more redox pairs of $Mn^{4+}/Mn^{3+}$ and $Fe^{3+}/Fe^{2+}$, which in turn enhance the oxidation reaction and generate additional reactive sites for the conversion of VOCs into $CO_2$ and $H_2O$ [18]. Therefore, FeO-$MnO_x$/OMS-2 was chosen for further experiments because it has high catalytic activity for the removal of WS. Figure 4(b) shows the effect of the calcination temperature (from 300 to 500 °C) on WS removal by oxidation. The removal of WS increased with increasing calcination temperature. However, the WS removal efficiency no longer increased when the calcination temperature increased to 500 °C. Therefore, a calcination temperature of 400 °C was suitable for the following experiments.

Figure 4(c) shows the removal efficiency of WS at different gas hourly space velocities (GHSV) over the catalyst. The experimental results demonstrated that WS removal decreased progressively from 95.9% to 74.0% as the GHSV increased from 9,947 to 39,789 $h^{-1}$. Higher GHSV values reduce the residence time of reactants in the catalyst bed, thereby lowering the overall oxidation efficiency. In contrast, lower GHSV values correspond to longer contact times, which enhances the interaction between the pollutant and active catalytic sites, thus promoting higher WS removal efficiency. The most significant drop in WS conversion was observed when the GHSV increased beyond 19,894 $h^{-1}$, suggesting a transition from a kinetically controlled regime to a diffusion-limited regime.

In real engineering applications, the concentrations of VOCs from various emission sources exhibit significant variability. The total number of active sites on the catalyst surface often limits the initial concentration of VOCs that can be effectively oxidized under fixed conditions. In a heterogeneous catalytic reaction, if the initial concentration is too low, the adsorption rate will affect the reaction rate, with chemical adsorption being the primary limiting factor. When the initial concentration is excessively high, the adsorption rate surpasses the reaction rate, making the surface reaction and desorption rates the critical factors. When the adsorption rate approximates the reaction rate, the initial concentration of VOCs is optimal, which results in the best removal efficiency [33]. The findings of this investigation are consistent with those of other studies, indicating that increasing the concentration reduces the removal efficiency of WS. Figure 4(d) depicts the results for different input WS concentrations while sustaining a flow rate of 1 L $min^{-1}$. As the WS concentration increased from 500 to 2,000 ppm, the removal efficiency increased from 80.3% to 96.9%. However, the efficiency decreased to 94.6% at a WS concentration of 2,500 ppm. At a low concentration of 500 ppm, WS molecules are insufficient to effectively use all the active sites of the catalyst [18, 34]. At a high concentration of 2,500 ppm, the adsorption surpasses the catalytic capability, thereby resulting in a slight decrease in removal efficiency.

Figure 4(e) shows the results when the FeO-$MnO_x$/OMS-2 catalyst with various masses from 0.5 to 2 g was used. The test was carried out with 2,000 ppm WS at the inlet concentration and a 1 L $min^{-1}$ gas flow rate. The removal efficiency reached 91.4% when 0.5 g of catalyst was used. The removal efficiency did not change appreciably when the catalyst mass ranged from 1 to 2 g. Hence, the use of 1 g of FeO-$MnO_x$/OMS-2 catalyst resulted in the highest removal efficiency of 96.7%.

The endurance of catalyst materials is one of the crucial criteria for their practical application. The durability test for the FeO-$MnO_x$/OMS-2 catalyst, as depicted in Figure 4(f), indicates that the catalyst exhibited a consistently high WS removal efficiency over the initial 4-hour period (ranging from 92.2% to 98.9%) when operated at a temperature of 200 °C, a flow rate of 1 L $min^{-1}$, and a concentration of 2,000 ppm. Nevertheless, after a duration of 4 h, the removal efficiency notably decreased from 90.8% to 60.0%, which can be attributed to the oxidation of iron oxide at high temperatures. These results suggest that while FeO-$MnO_x$/OMS-2 exhibited satisfactory performance in the initial treatment, its long-term durability for VOC treatment applications needs to be improved.

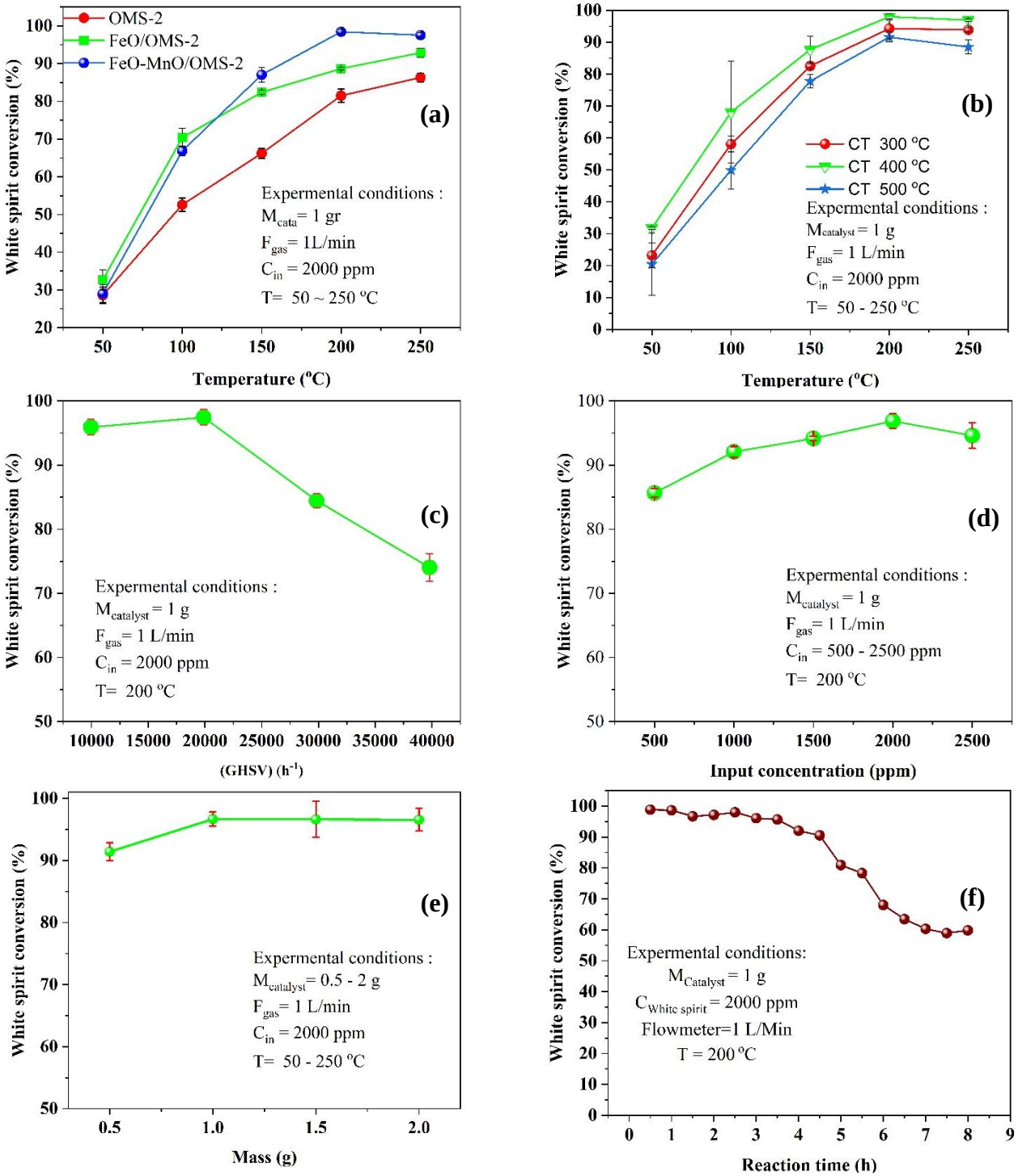


**Figure 4** Effect of (a) various catalyst materials, (b) material calcination temperatures, (c)GHSVs, (d) input concentrations, (e) catalyst masses. and (f) reaction times on the oxidation of white spirit vapor.

## Conclusion

Among the synthesized catalysts based on the OMS-2 material, FeO-$MnO_x$/OMS-2, with a surface Fe:Mn molar ratio of 6:4, exhibited high catalytic performance for WS oxidation. A suitable condition for the catalytic reaction was found, in which 1 g of FeO-$MnO_x$/OMS-2 was effective for the oxidation of 2000 ppm WS at a gas flow rate of 1 L $min^{-1}$, with a high WS removal efficiency of 97.91% at 200 °C. These results indicate the potential applicability of FeO-$MnO_x$/OMS-2 in WS oxidation, which is also promising for other VOC treatments. However, the catalyst was found to have limited long-term stability, which restricts its practical application without further improvements in durability.

## Acknowledgement

This research is funded by Vietnam National University – Ho Chi Minh City under grant number C2023-20-14. We acknowledge Ho Chi Minh City University of Technology (HCMUT), VNU-HCM for this study.

## References

[1] Pérez-Pastenes, H., Viveros-García, T. A new insight over oxygen storage capacity, SMSI, and dispersion effects on VOC oxidation using Pt/$Al_2O_3$–$CeO_2$ catalysts. Topics in Catalysis, 2022, 65(13–16), 1530–40.

[2] Abbasi, Z., Haghighi, M., Fatehifar, E., Saedy, S. Synthesis and physicochemical characterizations of nanostructured Pt/$Al_2O_3$–$CeO_2$ catalysts for total oxidation of VOCs. Journal of Hazardous Materials, 2011, 186(2), 1445–1454.

[3] Assal, M.E., Kuniyil, M., Khan, M., Al-Warthan, A., Siddiqui, M.R., Tremel, W. . . . Adil, S.F. Synthesis and comparative catalytic study of zirconia-$MnCO_3$ or -$Mn_2CO_3$ for the oxidation of Benzylic Alcohols. ChemistryOpen, 2017, 6(1), 112–120.

[4] Napruszewska, B., Michalik, A., Walczyk, A., Duraczyńska, D., Dula, R., Rojek, W. . . . Serwicka, E. Composites of laponite and Cu–Mn hopcalite-related mixed oxides prepared from inverse microemulsions as catalysts for total oxidation of toluene. Materials, 2018, 11, 1365.

[5] Kamal, M.S., Razzak, S.A., Hossain, M.M. Catalytic oxidation of volatile organic compounds (VOCs) – A review. Atmospheric Environment, 2016, 140, 117–134.

[6] Bourgeois, M., Guth, K., Harbison, R.D. Chemicals: Solvents. Information Resources in Toxicology: Elsevier; 2020. p. 221–228.

[7] Winchell, L.J., Ross, J.J., Brose, D.A., Pluth, T.B., Fonoll, X., Norton, J.W., Jr., Bell, K.Y. High-temperature technology survey and comparison among incineration, pyrolysis, and gasification systems for water resource recovery facilities. Water Environment Research, 2022, 94(4), e10715.

[8] Deng, H., Lu, Y., Pan, T., Wang, L., Zhang, C., He, H. Metals incorporated into OMS-2 lattice create flexible catalysts with highly efficient activity in VOCs combustion. Applied Catalysis B: Environmental, 2023, 320, 121955.

[9] Zhu, J., Cheng, Y., Wang, Z., Zhang, J., Yue, Y., Qian, G. Low-energy production of a monolithic catalyst with MnCu-synergetic enhancement for catalytic oxidation of volatile organic compounds. Journal of Environment Management, 2023, 336, 117688.

[10] Soltan, W.B., Sun, J., Wang, W., Song, Z., Zhao, X., Mao, Y., Zhang, Z. Discovering the key role of $MnO_2$ and $CeO_2$ particles in the $Fe_2O_3$ catalysts for enhancing the catalytic oxidation of VOC: Synergistic effect of the lattice oxygen species and surface-adsorbed oxygen. Science of the Total Environment, 2022, 819, 152844.

[11] Wang, Y., Yang, D., Li, S., Zhang, L., Zheng, G., Guo, L. Layered copper manganese oxide for the efficient catalytic CO and VOCs oxidation. Chemical Engineering Journal, 2019, 357, 258–268.

[12] Saqer, S.M., Kondarides, D.I., Verykios, X.E. Catalytic oxidation of toluene over binary mixtures of copper, manganese and cerium oxides supported on γ-$Al_2O_3$. Applied Catalysis B: Environmental, 2011, 103(3–4), 275–286.

[13] Genuino, H.C., Dharmarathna, S., Njagi, E.C., Mei, M.C., Suib, S.L. Gas-phase total oxidation of benzene, toluene, ethylbenzene, and xylenes using shape-selective manganese oxide and copper manganese oxide catalysts. The Journal of Physical Chemistry C, 2012, 116(22), 12066–12078.

[14] Aguero, F.N., Scian, A., Barbero, B.P., Cadús, L.E. Combustion of volatile organic compounds over supported manganese oxide: Influence of the support, the precursor and the manganese loading. Catalysis Today, 2008, 133–135, 493–501.

[15] Giang, L.T.H., Loc, L.C., Thoang, H.S. Investigation of physico-chemical properties of metallic oxide catalysts for complete oxidation. CTU Journal of Science, 2008, 10, 41–50.

[16] Wang, C.H., Lin, S.S., Chen, C.L., Weng, H.S. Performance of the supported copper oxide catalysts for the catalytic incineration of aromatic hydrocarbons. Chemosphere, 2006, 64(3), 503–509.

[17] Liu, X.S., Jin, Z.N., Lu, J.Q., Wang, X.X., Luo, M.F. Highly active CuO/OMS-2 catalysts for low-temperature CO oxidation. Chemical Engineering Journal, 2010, 162(1), 151-7.]

[18] Tang, H., Wu, S., Ding, L., Fang, N., Zhang, Q., Chu, Y. Catalytic oxidation and mixed oxidation of ethyl acetate: A review. Separation and Purification Technology, 2024, 343, 126980.

[19] Li, M., Zhang, X., Liu, X., Lian, Y., Niu, X., Zhu, Y. Excellent low-temperature activity for oxidation of benzene serials VOCs over hollow Pt/$CoMn_2O_4$ sub-nanosphere: Synergistic effect between Pt and $CoMn_2O_4$ on improving oxygen activation. Chemical Engineering Journal, 2023, 473, 145478.

[20] Einaga, H., Yamamoto, S., Maeda, N., Teraoka, Y. Structural analysis of manganese oxides supported on $SiO_2$ for benzene oxidation with ozone. Catalysis Today, 2015, 242, 287–293.

[21] Luo, J., Zhang, Q., Huang, A., Suib, S.L. Total oxidation of volatile organic compounds with hydrophobic cryptomelane-type octahedral molecular sieves. Microporous and Mesoporous Materials, 2000, 35, 209-17.

[22] Sun, Q., Li, L., Yan, H., Hong, X., Hui, K.S., Pan, Z. Influence of the surface hydroxyl groups of $MnO_x$/SBA-15 on heterogeneous catalytic ozonation of oxalic acid. Chemical Engineering Journal, 2014, 242, 348–356.

[23] Hien, T.T.T., Hiep, V.D., Chuc, N.V., Hung, K.M., Thuy, L.B., Thang, L.M. Determination of the potential byproduct in the toluene oxidation process by $CuMnO_x$ catalyst on cordierite substrate. Vietnam Journal of Catalysis and Adsorption, 2022, 11(3), 1–7.

[24] Behar, S., Gonzalez, P., Agulhon, P., Quignard, F., Świerczyński, D. New synthesis of nanosized Cu–Mn spinels as efficient oxidation catalysts. Catalysis Today, 2012, 189(1), 35–41.

[25] Morales, M.R., Barbero, B.P., Cadús, L.E. Total oxidation of ethanol and propane over Mn-Cu mixed oxide catalysts. Applied Catalysis B: Environmental, 2006, 67(3), 229–236.

[26] Pérez, H., Navarro, P., Delgado, J.J., Montes, M. Mn-SBA15 catalysts prepared by impregnation: Influence of the manganese precursor. Applied Catalysis A: General, 2011, 400(1), 238–248.

[27] Zhang, J., Zhang, C., He, H. Remarkable promotion effect of trace sulfation on OMS-2 nanorod catalysts for the catalytic combustion of ethanol. Journal of Environmental Sciences, 2015, 35, 69–75.

[28] Ren, L., Feng, N., Yu, J., Zhao, P., Zhang, X., Wan, H., Guan, G. Modulated synthesis of $MnO_2$-decorated Fe–Mn composite oxides : synergistic effects on boosting the performance of toluene oxidation. Journal of Solid State Chemistry, 2023, 326, 124244.

[29] Nguyen, N.H., Ngo, Q., Duy, H., Hang, V., Thuy, N., Thanh, V.TT. Low-temperature catalytic oxidation of white spirit vapor in air by binary oxides of $CuO$-$MnO_x$ supported on OMS-2 material. Suranaree Journal of Science and Technology, 2025, 31, 030237(1–7).

[30] Olkhovskaya, Z.K. Colorimetric method for assaying the hydrocarbons, benzene, Kerosene, and white spirit in the air of industrial installations. Olkhovskaya, ZK; 1971. Report No.: NIOSH/0074146.

[31] Zeng, J., Liu, X., Wang, J., Lv, H., Zhu, T. Catalytic oxidation of benzene over MnOx/$TiO_2$ catalysts and the mechanism study. Journal of Molecular Catalysis A: Chemical, 2015, 408, 221–227.

[32] Moreno-Román, E.J., Can, F., Meille, V., Guilhaume, N., González-Cobos, J., Gil, S. MnOx catalysts supported on SBA-15 and MCM-41 silicas for a competitive VOCs mixture oxidation: In-situ DRIFTS investigations. Applied Catalysis B: Environment and Energy, 2024, 344, 123613.

[33] Zhao, R., Wang, H., Zhao, D., Liu, R., Liu, S., Fu, J. . . . Ding, H. Review on catalytic oxidation of VOCs at ambient temperature. International Journal of Molecular Sciences, 2022, 23(22).

[34] Yadav, M., Pophali, A., Verma, N., Kim, T. Oxidation of VOCs on a highly stabilized furfuryl alcohol-based activated carbon supported nickel oxide catalyst. Journal of Industrial and Engineering Chemistry, 2022, 105, 313–323.